

# Tumor-Derived Extracellular Mutations of PTPRT/PTP $\rho$ Are Defective in Cell Adhesion

Jianshi Yu,<sup>1,2</sup> Scott Becka,<sup>3</sup> Peng Zhang,<sup>2</sup> Xiaodong Zhang,<sup>1,2</sup>  
Susann M. Brady-Kalnay,<sup>1,3,4</sup> and Zhenghe Wang<sup>1,2,5</sup>

<sup>1</sup>Case Comprehensive Cancer Center and Departments of <sup>2</sup>Genetics, <sup>3</sup>Molecular Biology and Microbiology, and <sup>4</sup>Neurosciences, School of Medicine, Case Western Reserve University; and <sup>5</sup>Genomic Medicine Institute, Cleveland Clinic Foundation, Cleveland, Ohio

## Abstract

Receptor protein tyrosine phosphatase T (PTPRT/PTP $\rho$ ) is frequently mutated in human cancers including colon, lung, gastric, and skin cancers. More than half of the identified tumor-derived mutations are located in the extracellular part of PTP $\rho$ . However, the functional significance of those extracellular domain mutations remains to be defined. Here we report that the extracellular domain of PTP $\rho$  mediates homophilic cell-cell aggregation. This homophilic interaction is very specific because PTP $\rho$  does not interact with its closest homologue, PTP $\mu$ , in a cell aggregation assay. We further showed that all five tumor-derived mutations located in the NH<sub>2</sub>-terminal MAM and immunoglobulin domains impair, to varying extents, their ability to form cell aggregates, indicating that those mutations are loss-of-function mutations. Our results suggest that PTP $\rho$  may play an important role in cell-cell adhesion and that mutational inactivation of this phosphatase could promote tumor migration and metastasis. (Mol Cancer Res 2008;6(7):1106–13)

## Introduction

Tyrosine phosphorylation is coordinately controlled by protein tyrosine kinases and phosphatases and is a central feature of many signaling pathways involved in tumor development (1). Whereas activating mutations in protein tyrosine kinases have been shown to play vital roles in tumorigenesis (1), the role of phosphatases is less well defined. We recently identified PTPRT, also known as PTP $\rho$ , as the most frequently mutated PTP gene in colorectal cancers (2). PTPRT was also mutationally altered in lung cancer, gastric cancer, and melanomas (2). The spectrum of mutations, which included

nonsense mutations and frameshifts, suggested that these mutations were inactivating (2). Biochemical analyses showed that missense mutations in the catalytic domains of PTP $\rho$  diminished its phosphatase activity, and overexpression of PTP $\rho$  inhibited colorectal cancer cell growth (2). Taken together, these studies strongly supported the notion that PTP $\rho$  normally acts as a tumor suppressor gene. This conclusion was also supported by a transposon-based somatic mutagenesis screen in mice, in which PTP $\rho$  was isolated as a target gene from two different mouse transgenic sarcomas (3).

PTPRT (PTP $\rho$ ) is a member of the type IIB receptor protein tyrosine phosphatase (RTP) subfamily (4). Other members of this subfamily include PTPRM (PTP $\mu$ ), PTPRK (PTP $\kappa$ ), and PCP2 (also called PTP $\lambda$ , PTP $\psi$ , PTPRO-omicron, PTP $\pi$ , or hPTP-J; ref. 5). These four RTPs share the same domain structure: an extracellular domain, a juxtamembrane region, and two phosphatase domains (6). The extracellular domains of type IIB RTPs have high sequence identities (6–8), all consisting of a MAM (memprin/A5/PTP $\mu$ ) domain, an immunoglobulin domain, and four fibronectin type III repeats (6). The MAM domain is suggested to play a role in protein dimerization (6). The immunoglobulin domain is a disulfide structure that is found in many cell surface proteins and has been shown to mediate homophilic and heterophilic interactions between cell adhesion molecules (6). The fibronectin type III motif was originally identified in the extracellular matrix protein fibronectin and later found to be present in many immunoglobulin superfamily cell adhesion molecules (6). We have identified ~15 somatic mutations that are localized in the extracellular domain of PTPRT/PTP $\rho$ . How these mutations affect the functions of PTP $\rho$  remains to be determined.

Three close homologues of PTP $\rho$  [PTP $\mu$ , PTP $\kappa$ , and PTP $\lambda$  (PCP-2)] are known to mediate homophilic cell-cell adhesion (9–12). Expression of the full-length PTP $\mu$  (9, 10) or a construct encoding the extracellular, transmembrane, and 55 amino acids of the juxtamembrane domain of PTP $\mu$  in nonadhesive Sf9 insect cells induces cell aggregation (9). Furthermore, homophilic binding of PTP $\mu$  was shown between PTP $\mu$ -coated fluorescent beads and cells that endogenously express PTP $\mu$  (9). The minimal region required for homophilic binding was mapped to the immunoglobulin domain of PTP $\mu$  (13). In addition, the immunoglobulin domain is required for proper cell surface localization (14). However, assays that test cell-cell aggregation show that the MAM and immunoglobulin domains as well as the first two fibronectin type III repeats are required for efficient cell-cell aggregation (15–18). Similarly, PTP $\kappa$  was also shown to mediate homophilic cell-cell aggregation (11).

Received 10/29/07; revised 2/29/08; accepted 4/9/08.

**Grant support:** NIH grants R01-CA127590 and U54CA116867 (Z. Wang) and grants R01-EY12251 and R01-NS051520 (S.M. Brady-Kalnay), the Concern Foundation, the V Foundation (Z. Wang), and Visual Sciences Research Center Core Grant PO-EY11373 from the National Eye Institute (S.M. Brady-Kalnay). The costs of publication of this article were defrayed in part by the payment of page charges. This article must therefore be hereby marked *advertisement* in accordance with 18 U.S.C. Section 1734 solely to indicate this fact.

**Requests for reprints:** Zhenghe Wang, Department of Genetics and Case Comprehensive Cancer Center, Case Western Reserve University, Wolstein Research Building 3-120, 10900 Euclid Avenue, Cleveland, OH 44106. Phone: 216-368-0446; Fax: 216-368-8919. E-mail: zhenghe.wang@case.edu  
Copyright © 2008 American Association for Cancer Research.  
doi:10.1158/1541-7786.MCR-07-2123

Here we report that PTPRT (PTP $\rho$ ), like its homologues, mediates homophilic cell-cell aggregation in Sf9 cells. Most importantly, the tumor-derived mutations located in the MAM and immunoglobulin domains cause defective cell-cell adhesion function.

## Results

### The Extracellular Domain of PTP $\rho$ Mediates Cell-Cell Aggregation in Sf9 Cells

To test whether PTP $\rho$  mediates homophilic cell-cell adhesion, we made PTP $\rho$  baculoviral constructs expressing (a) full-length PTP $\rho$ ; (b) the intracellular fragment of PTP $\rho$  (Intra); (c) the extracellular fragment of PTP $\rho$  with its transmembrane domain (Extra-TM); (d) the extracellular fragment of PTP $\rho$  with its transmembrane, juxtamembrane, and wedge domains (Extra-JMD-W); and (e) a chimera containing the extracellular and transmembrane domains of the epidermal growth factor receptor and the intracellular PTP domains of PTP $\rho$  (Fig. 1A). All of those fragments were tagged with V5 epitope tags. Proteins of the expected size were expressed in Sf9 cells infected with those baculoviral constructs (Fig. 1B). All of these proteins, but the intracellular PTP $\rho$ , were expressed on the surface on Sf9 cells (Figs. 1C and 7). To test whether these PTP $\rho$  recombinant proteins mediate cell-cell adhesion, a cell aggregation assay was done following the procedure of Brady-Kalnay et al. (9). Sf9 cells infected with a baculovirus encoding PTP $\mu$ , which was previously shown to mediate cell-cell aggregation, were treated in parallel as a positive control (Fig. 2). As shown in Fig. 2, the nonadhesive Sf9 cells expressing either the full-length PTP $\rho$  or PTP $\rho$ -JMD-W formed cell aggregates. On the contrary, Sf9 cells expressing either the intracellular fragments of PTP $\rho$  or the epidermal growth factor receptor/PTP $\rho$  chimeras remained as a suspen-

sion of single cells (Fig. 2). These results indicate that the extracellular fragment of PTP $\rho$  plays an important role in mediating cell-cell aggregation and that the phosphatase activity of PTP $\rho$  is not required for this function. Surprisingly, although the construct that encodes the PTP $\rho$  extracellular fragment with the transmembrane domain sequences only (Extra-TM) was expressed on the cell surface (see Fig. 7), this protein failed to mediate cell aggregation of Sf9 cells (Fig. 2), suggesting that additional juxtamembrane sequences are required for either forming or stabilizing the cell aggregates.

### PTP $\rho$ Mediates Highly Specific Homophilic Cell-Cell Aggregation

To test whether PTP $\rho$  mediates homophilic cell-cell aggregation, one set of Sf9 cells was infected with viruses expressing enhanced green fluorescent protein and another set of Sf9 cells was coinfecting with viruses expressing the full-length PTP $\rho$  and red fluorescent protein. The green fluorescent protein-expressing cells were mixed with equal number of cells expressing full-length PTP $\rho$  (coexpressing red fluorescent protein) and the aggregation assays were done. As shown in Fig. 3A, the green fluorescent protein-labeled cells did not aggregate and did not contribute to the aggregates formed by cells expressing full-length PTP $\rho$  (red fluorescent protein). These results strongly suggest that the aggregation of Sf9 cells expressing PTP $\rho$  is mediated through a homophilic interaction among PTP $\rho$  molecules in *trans*, but not through a heterophilic interaction between molecules expressed on the surface of Sf9 cells. Interestingly, the homophilic interaction of PTP $\rho$  is very specific. Although 63% of the amino acid sequences of the extracellular domain of PTP $\rho$  are identical with that of PTPRM (PTP $\mu$ ), Sf9 cells expressing PTP $\rho$  (coexpressing red fluorescent protein) did not aggregate with

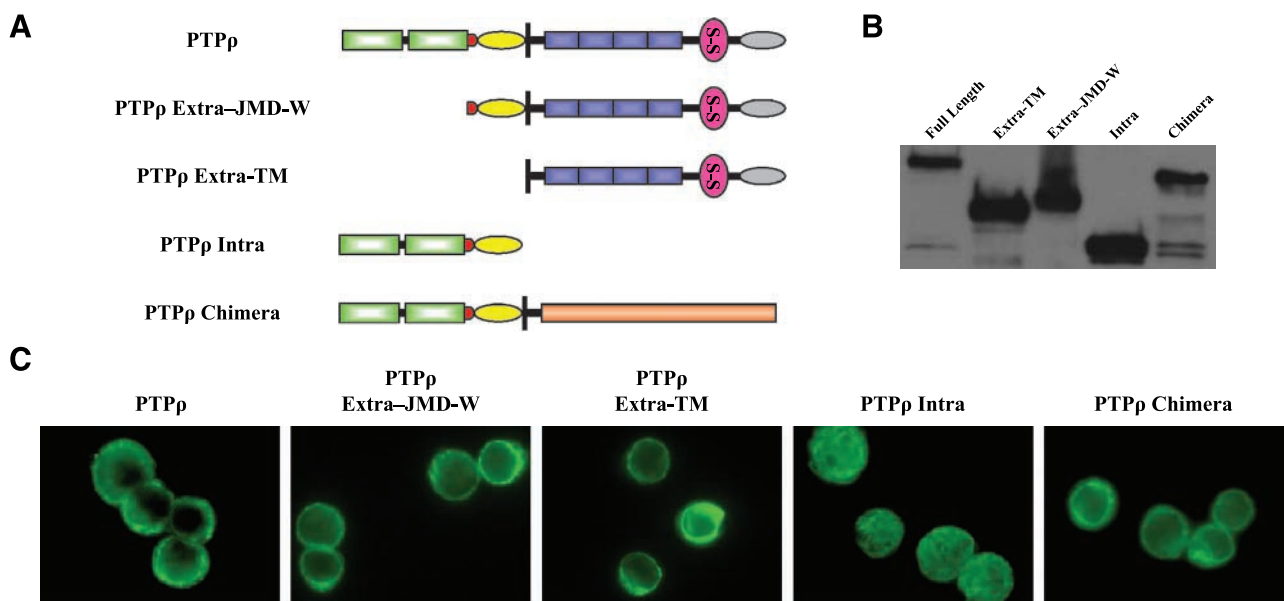


**FIGURE 1.** Expression of PTP $\rho$  constructs in Sf9 cells. **A.** Schematic diagram of PTP $\rho$  constructs. Gray oval, MAM domain; pink circle, immunoglobulin domain; yellow oval, juxtamembrane domain; red circle, Wedge domain; green rectangles, phosphatase domain. **B.** Western blot of lysates from Sf9 cells expressing the indicated PTP $\rho$  constructs. **C.** Immunofluorescent staining of Sf9 cells expressing the indicated PTP $\rho$  proteins.

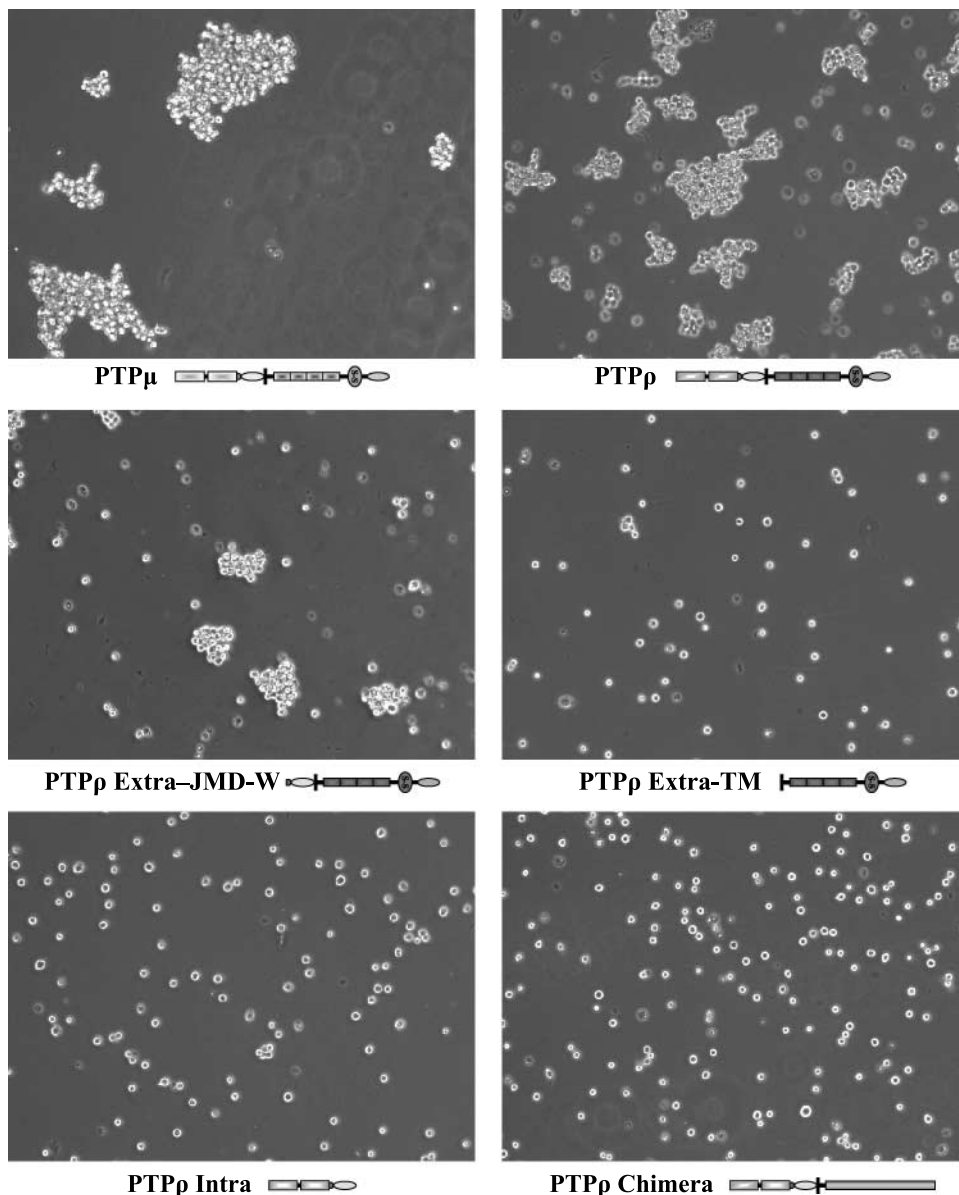


**FIGURE 2.** PTP $\rho$  mediates cell-cell aggregation. Sf9 cells were infected with the indicated baculoviral constructs for 48 h. Cell aggregation assay was done under low shear conditions and representative phase images were captured with a microscope.

PTP $\mu$ -expressing cells (coexpressing green fluorescent protein), as shown in Fig. 3B.

*The Tumor-Derived PTPRT/PTP $\rho$  Mutations in the MAM and Immunoglobulin Domains Result in Defective Cell-Cell Aggregation*

Several studies showed that the MAM and immunoglobulin domains as well as the first two fibronectin type III repeats of PTP $\mu$  are the minimal essential regions required for its homophilic interaction (13, 15, 17, 18). We identified five tumor-specific mutations that are located in the two domains (2). Among these five mutations, the F74S mutation is located in the MAM domain and the other four mutations (A209T, K218T, F248S, and Y280H) are located in the immunoglobulin domain (Fig. 4A). To test whether these mutations affect their ability to mediate cell-cell aggregation in Sf9 cells, we

engineered the five mutations by site-directed mutagenesis using the full-length PTP $\rho$  baculoviral construct as the template. The five mutant proteins are expressed at the expected size and at similar levels to wild-type PTP $\rho$  on a Western blot (Fig. 4B), indicating that these mutations do not affect their protein stability. None of these mutations significantly alter their cell surface expression because all five mutant PTP $\rho$  proteins showed strong plasma membrane staining and cell surface labeling (Figs. 4C and 7). However, as shown in Fig. 5, all mutant PTP $\rho$  proteins formed smaller aggregates than that of the wild-type PTP $\rho$  protein. To quantify the cell aggregates, the percentage of cells that are incorporated into >5-cell clusters was counted (as described in Materials and Methods). As shown in Fig. 6, Sf9 cells expressing all the mutants formed significantly less aggregates than did the cells expressing wild-type PTP $\rho$ . The deletion construct of PTP $\rho$

lacking the two phosphatase domains (PTP $\rho$  Extra-JMD-W) and the K218T mutant exhibited similar levels of aggregation that were statistically less than wild-type PTP $\rho$  ( $P < 0.01$ ). Taken together, our data showed that the five tumor-derived mutations located in the MAM and immunoglobulin domains of PTP $\rho$  cause defective cell-cell adhesion. Therefore, these mutations exhibit varying degrees of loss-of-function in cell adhesion.

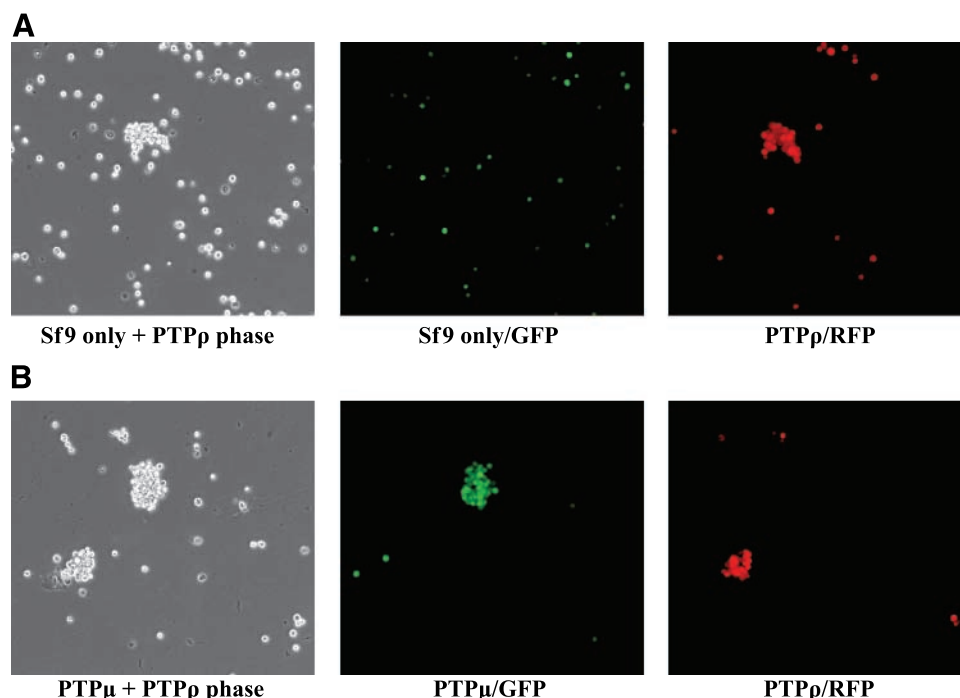
Mechanistically, the defect in cell-cell adhesion caused by the PTP $\rho$  mutations could have resulted from either impaired homophilic binding or reduced cell surface expression. Although immunofluorescent staining indicated that those mutations do not alter cell surface expression qualitatively, it is imperative to quantify cell surface expression of mutant PTP $\rho$  proteins. As described in detail in Materials and Methods, baculovirus-infected Sf9 cell surface proteins were labeled with Sulfo-NHS-SS-Biotin and isolated on immobilized NeutrAvidin gel. Western blots were done with antibodies to PTP $\mu$  (SK18) or the V5 tag. The SK18 antibody recognizes the cytoplasmic domain of both PTP $\mu$  and PTP $\rho$ . The results shown in Fig. 7 show that full-length PTP $\mu$  and the wild-type, mutant, and deleted PTP $\rho$  proteins were expressed at the cell surface. As a control for a non-cell-surface protein, the cytoplasmic intracellular domain of PTP $\mu$  (PTP $\mu$  Intra) was expressed, which is detected by SK18 (9). PTP $\mu$  Intra does not contain an extracellular domain and therefore is not biotinylated or precipitated by the NeutrAvidin gel (Fig. 7). Quantitatively, the levels of cell surface expression of the five tumor-derived PTP $\rho$  mutations were similar to that of wild-type protein. If the cell surface expression level (cell surface expression value) of wild-type PTP $\rho$  is arbitrarily assigned as 1, the cell surface expression values of F74S, A209T, K218T, F248S, and Y280H mutations were 2.3, 1.1, 1.6, 0.6, and 0.8 respectively. Interestingly, some PTP $\rho$  mutants that contain the extracellular

domain but are unable to mediate cell-cell aggregation are expressed at higher levels on the Sf9 cell surface than wild-type PTP $\rho$ . These results suggest that the defect caused by PTP $\rho$  mutation in cell-cell adhesion is mainly due to reduced homophilic binding affinity of the mutant proteins. Interestingly, the cell surface expression levels PTP $\rho$  Extra-TM (cell surface expression value, 27) and PTP $\rho$  Extra-JMD-W (cell surface expression value, 20) were much higher than that of full-length protein for unknown reasons.

## Discussion

We showed that PTPRT/PTP $\rho$  mediates homophilic cell-cell aggregation and five tumor-derived mutations located in the MAM and immunoglobulin domains impair this function. Our results strongly suggest that those PTP $\rho$  loss-of-function mutations are selected for during the process of tumor development; therefore, these mutations should play a causal role in tumorigenesis. We chose to examine whether the MAM and immunoglobulin domain mutations are defective in cell aggregation because previous studies indicated that these two domains of PTP $\mu$ , a close homologue of PTP $\rho$ , are required for its cell-cell aggregation function (13, 15, 17). Recently, the crystal structure of the NH<sub>2</sub>-terminal MAM and immunoglobulin domains of PTP $\mu$  was determined at 2.7-Å resolution (17, 18). Five tumor-derived mutations of PTP $\rho$  are located in the two domains and all of them can be mapped to equivalent residues in the MAM and immunoglobulin domain structure of PTP $\mu$ . Based on the crystal structure, the authors predicted that four of them (F74S, A209T, F248S, and Y280H) would cause significant perturbation of the structure of PTPRT because these mutations dramatically alter the character of buried side chains (17). Moreover, the fifth mutation K218T is located on the surface of the immunoglobulin domain and the authors

**FIGURE 3.** PTP $\rho$  mediates homophilic cell-cell aggregation. **A.** Sf9 cells were infected with green fluorescent protein (GFP), whereas another flask of Sf9 cells was coinfecting with PTP $\rho$  and red fluorescent protein (RFP) viruses. Sf9 cells from the two flasks were mixed at 1:1 ratio and a cell aggregation assay was done. **B.** One flask of Sf9 cells was coinfecting with PTP $\mu$  and green fluorescent protein viruses, whereas another flask of Sf9 cells was coinfecting with PTP $\rho$  and red fluorescent protein viruses. Sf9 cells from the two flasks were mixed at 1:1 ratio and a cell aggregation assay was done. Images of cell aggregates were captured under phase, green fluorescent protein, and red fluorescent protein filters, respectively.



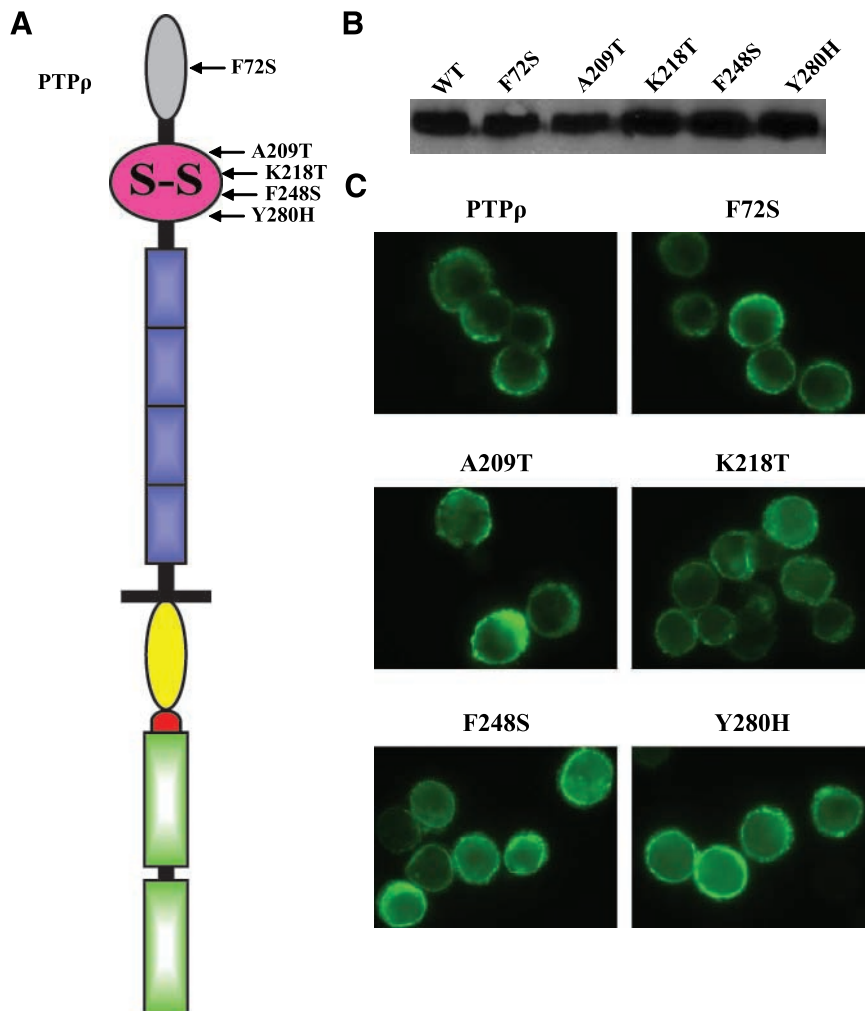


**FIGURE 4.** Expression of tumor-derived PTP $\rho$  mutants in Sf9 cells. **A.** Schematic diagram of PTP $\rho$  mutations located in the MAM and immunoglobulin domains. **B.** Western blot of lysates from Sf9 cells expressing the indicated PTP $\rho$  mutations. **C.** Immunofluorescent staining of Sf9 cells expressing the indicated PTP $\rho$  mutant proteins.

predicted that this mutation would directly alter protein-protein interactions (17). Our data indicated that the K218T mutation affects the size of aggregates and has only a small effect on the percentage of cells incorporated into the aggregates, suggesting that the K218T mutant may decrease the binding affinity of PTP $\rho$ . Interestingly, the other four mutations significantly reduce the percentage of aggregation; therefore, these data suggest that the F74S, A209T, F248S, and Y280H mutations dramatically alter the domain structure and lead to perturbation of the homophilic interaction of PTP $\rho$ . Our previous studies showed that the tumor-derived phosphatase domain mutations of PTP $\rho$  diminish its phosphatase activity, and overexpression of PTP $\rho$  suppresses the growth of colorectal cancer cells, indicating that PTP $\rho$  normally acts as a tumor suppressor (2). The loss-of-function nature of these five extracellular mutations provides further supportive evidence to this notion.

The finding that PTP $\rho$  mediates homophilic cell aggregation of nonadhesive insect Sf9 cells suggests that this protein could be involved in cell-cell adhesion in human epithelial cells where it is endogenously expressed. The type IIB RPTP subfamily consists of PTP $\mu$ , PTP $\kappa$ , PTP $\rho$ , and PCP-2. It has been shown that PTP $\mu$ , PTP $\kappa$ , and PTP $\lambda$  (PCP-2) mediate

homophilic cell-cell adhesion (9-12). Interestingly, the homophilic interaction of these RPTPs seems to be highly specific because we and others showed that neither PTP $\rho$  nor PTP $\kappa$  (15) interacts with PTP $\mu$ . It is worth noting that the juxtamembrane domain of PTP $\rho$  may be necessary for its cell adhesion function. As shown in Fig. 2, Sf9 cells expressing the extracellular and juxtamembrane domains of PTP $\rho$ , but not cells expressing the extracellular and transmembrane portion of the protein (PTP $\rho$  Extra-TM), formed cell aggregates, although both proteins were expressed on the cell surface (Fig. 7). Expression of a construct encoding the extracellular, transmembrane, and only 55 amino acids of the juxtamembrane domain of PTP $\mu$  in nonadhesive Sf9 insect cells induced cell aggregation (9). It is possible that *cis* interactions between the membrane proximal juxtamembrane domains are required for initiating, stabilizing, or maintaining cell-cell adhesion. Interestingly, there are two *PTPRT* mutations (K788E and R790I) located in the juxtamembrane domain that are found in lung cancers (1). Moreover, Besco et al. (19) showed that PTP $\rho$  interacts with cell adhesion molecules including E-cadherin,  $\alpha$ -catenin,  $\beta$ -catenin,  $\gamma$ -catenin, and  $\alpha$ -actinin. PTP $\mu$  also binds the cadherin-catenin complex (7, 20-22). Loss of cell-cell

adhesion, such as genetic and epigenetic inactivation of cell adhesion molecule E-cadherin, is thought to be a prerequisite for carcinoma invasion and metastasis (23). Therefore, mutational inactivation of the cell adhesion function PTP $\rho$  may also play a critical role in tumor migration and metastasis.

## Materials and Methods

### Cell Culture

Insect Sf9 cells (BD Biosciences) were maintained at 27°C in TNM-FH insect medium (BD Biosciences).

### Plasmid and Baculovirus Construction

To tag our protein of interest with a V5 tag, we first constructed a pVL1393-V5-His vector. A 450-bp fragment containing the V5 and 6xHis epitopes was digested with *Bam*HI and *Pme*I restriction enzymes from pcDNA3.1 and then

cloned into the pVL1393 vector cleavage by *Bam*HI and *Bg*II (blunt ended). The full-length PTPRT/PTP $\rho$  was inserted and in-frame fused with the V5 tag in the pVL1393-V5-His vector. PCR were used to generate the following constructs: PTP $\rho$  Intra (663 amino acids, bp 2,401-4,392), PTP $\rho$  Extra-TM (787 amino acids, bp 1-2,361) and PTP $\rho$  Extra-JMD-W (916 amino acids, bp 1-2,748). A chimera containing the extracellular and transmembrane domains of the epidermal growth factor receptor (673 amino acids, bp 170-2190) and the intracellular PTP domains of PTPRT (663 amino acids, bp 2401-4392) was generated by in-frame fusion of the epidermal growth factor receptor fragment with the PTP $\rho$  Intra construct. All constructs were sequenced to ensure that no mutations were introduced by PCR. These constructs were cotransfected with the BaculoGold Linearized Baculovirus DNA (BD Biosciences) according to the manufacturer's instructions to generate recombinant viruses. The PTP $\mu$  baculovirus has been described (9).

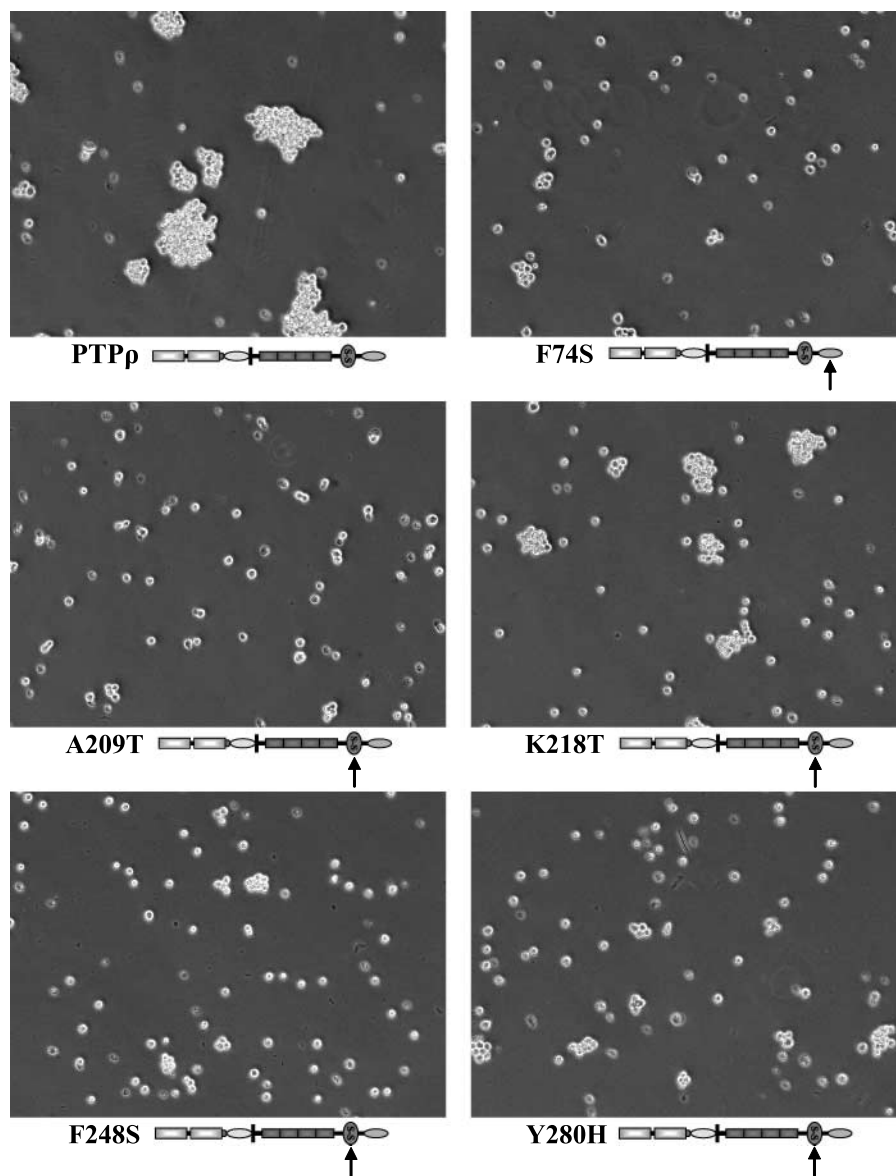


**FIGURE 5.** Tumor-derived mutations of PTP $\rho$  result in defective cell-cell aggregation. Cell aggregation assay of Sf9 cells expressing either wild-type or the indicated mutation of PTP $\rho$  was done under low shear conditions. Representative phase images were captured with a microscope.

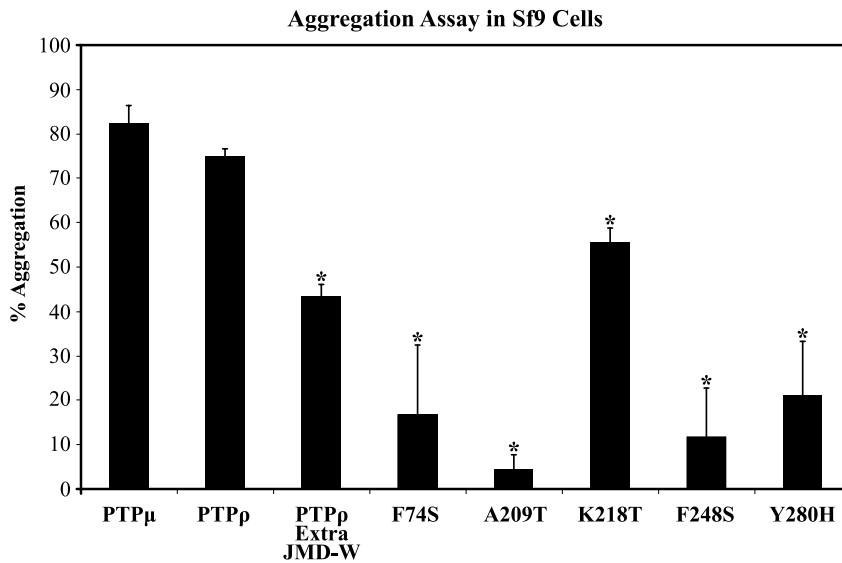


**FIGURE 6.** Quantification of the cell-cell aggregation assays. The percentage of aggregated Sf9 cells for each indicated protein was calculated from three independent experiments. \*,  $P < 0.01$ , between wild-type PTP $\rho$  and each of the mutants (Student's  $t$  test).

#### Sf9 Cell Aggregation Assays

The cell aggregation assays were done as previously described (9) with minor modifications. Sf9 cells were harvested 2 d postinfection. The cell suspensions were added to glass scintillation vials and incubated at 25°C at 90 rpm in a gyratory shaker for 30 min. For a given condition, half of the cell suspension was poured into a 100-mm Petri dish either before (0 time point) or after 30 min of aggregation. Images were captured with a Nikon inverted fluorescence microscope (TE-200). To quantify cell aggregates, 10 pictures of randomly selected fields were taken for each time point and condition in that experiment. The area of each object (single cells and aggregates) was determined with the Metamorph software (Molecular Devices) using a threshold setting of 160 and appropriate size filters that allowed the counting of cells and aggregates but not debris. The percentage of aggregation for an experiment was calculated as the average area at 30 min minus the average area at the zero time point divided by the average area at the 30-min time point ( $N_{30} - N_0 / N_{30}$ ). At least three independent experiments were done for each condition.

#### Western Blotting

Sf9 Cells were harvested 2 d postinfection and lysed in RIPA buffer [50 mmol/L Tris-HCl (pH 8.0), 0.5% Triton X-100, 0.25% sodium deoxycholate, 150 mmol/L sodium chloride, 1 mmol/L EDTA] with complete protease inhibitor cocktail. Western blots were done as described (24) with a mouse anti-V5 antibody (Invitrogen) or SK18 (9).

#### PTP $\rho$ Immunofluorescence

Sf9 cells were fixed with 4% paraformaldehyde for 30 min at room temperature and permeabilized with 0.2% Triton X-100 (diluted in PBS). Cells were blocked with Image-iT FX signal enhancer (Invitrogen) for 30 min and then stained with mouse anti-V5 antibody (Invitrogen) followed by an Alexa 488-conjugated secondary antibody (Invitrogen). Images were captured with a Nikon fluorescence microscope.

#### Site-Directed Mutagenesis

The F74S, A209T, K218T, F248S, and Y280H mutations were generated by fusion PCR (25) using the full-length PTPRT pVL1393-V5-His vector as the template. The primers GCAGTCCCCACAGGATCTTCCATGATGGTGAACAGCTCT and GAAGATCCTGTGGGCACTGC were used as the mutagenic primers for the F74S mutant; the primers GGTGAA-TGTGGGGCAGAATACCACATTTTCAGTGCATTGC and TATTCTGCCCCACATTCACC were used as the mutagenic primers for the A209T mutant; the primers CGTGGTCTCAGCATGACAAG and CTTGTCATGCTGAGACCACGTCCCA-CCAGCAATGCACTG were used as the mutagenic primers for the K218T mutant; the primers GTGGTCAACCACAGGCGC-TCCTCAGCCACAGTCAGTGTG and GAGCGCCTGTGGT-TGACCAC were used as the mutagenic primers for the F248S mutant; and the primers CACGCGGAGCTGATCGTGAA

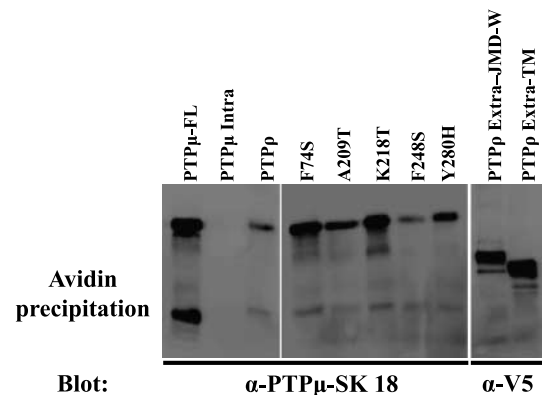


**FIGURE 7.** Cell surface protein expression of PTP $\mu$  and the PTP $\rho$  mutant proteins. The cell surface proteins were labeled with Sulfo-NHS-SS-Biotin. The biotinylated proteins were isolated on NeutrAvidin gel. The bound proteins were eluted, run on SDS-PAGE gels, transferred onto nitrocellulose, and immunoblotted with antibodies to PTP $\mu$  (SK18) or the V5 tag. The SK18 antibody recognizes the cytoplasmic domain of both PTP $\mu$  and PTP $\rho$ .

and TTCACGATCAGCTCCGCGTGGTTGGACACACCAG-ACCCA were used as the mutagenic primers for the Y280H mutant.

#### Quantification of Cell Surface Expression of PTP $\rho$ and PTP $\mu$ Proteins

The amount of PTP $\mu$  and the PTP $\rho$  proteins expressed at the Sf9 cell surface was determined using the Cell Surface Protein Isolation Kit (Pierce). The kit provides the proprietary reagents referred to below including wash buffer, lysis buffer, and the column. Sf9 cells were grown to 80% confluence in T25 flasks and infected with baculovirus as described above. Forty-eight hours postinfection, the medium was removed and 5 mL of 0.25 mg/mL Sulfo-NHS-SS-Biotin in 1 $\times$  PBS were added to each flask. The flasks were placed on a rocking platform for 30 min at 4°C. Quenching Solution (250  $\mu$ L) was added to each flask to quench the reaction. The cells were mechanically removed from the flask and centrifuged at 5,000 rpm for 3 min, washed, and centrifuged again. The cells were lysed by incubated on ice for 30 min with lysis buffer, vortexed, and centrifuged at 10,000 rpm for 2 min. Immobilized NeutrAvidin gel slurry (250  $\mu$ L) was added to the column. The column was washed thrice. The cell lysate was added to the column and incubated for 60 min at room temperature with rocking. The column was centrifuged for 1 min at 1,000 rpm and washed thrice. Two hundred microliters of sample buffer containing a final concentration of 55 mmol/L DTT were added to the gel and incubated for 60 min on a platform rocker at room temperature. The column was centrifuged for 2 min at 1,000 rpm and the flow-through was collected. The flow-through was run on 6% SDS-PAGE gels and transferred onto nitrocellulose. Total cell surface protein levels were normalized by immunoblotting with streptavidin-horseradish peroxidase (Jackson ImmunoResearch Laboratories, Inc.). The normalized cell surface protein was run on 6% SDS-PAGE gels, transferred onto nitrocellulose, and immunoblotted with antibodies to PTP $\mu$  (SK18) or the V5 tag followed by secondary antibody conjugated to horseradish peroxidase. The horseradish peroxidase signal was detected using a Fluor-S MAX MultiImager (Bio-Red Laboratories, Inc.). Horseradish peroxidase signal was quantitated by densitometry using the Quantity One Software from Bio-Rad. The densitometry in the results represents a comparison of the quantitation of the V5 signal for all PTP $\rho$  proteins with the number for wild-type PTP $\rho$ , which we assigned a value of 1. We define this value as the cell surface expression value.

#### Disclosure of Potential Conflicts of Interest

No potential conflicts of interest were disclosed.

#### Acknowledgments

We thank Drs. Sanford Markowitz and David Sedwick for helpful discussions and Sara Lou for the preparation of the figures and graphs.

#### References

1. Blume-Jensen P, Hunter T. Oncogenic kinase signalling. *Nature* 2001;411:355–65.

- Wang Z, Shen D, Parsons DW, et al. Mutational analysis of the tyrosine phosphatome in colorectal cancers. *Science* 2004;304:1164–6.
- Collier LS, Carlson CM, Ravimohan S, Dupuy AJ, Largaespa DA. Cancer gene discovery in solid tumours using transposon-based somatic mutagenesis in the mouse. *Nature* 2005;436:272–6.
- McAndrew PE, Frostholm A, White RA, Rotter A, Burghes AH. Identification and characterization of RPTP $\rho$ , a novel RPTP $\mu/\kappa$ -like receptor protein tyrosine phosphatase whose expression is restricted to the central nervous system. *Brain Res Mol Brain Res* 1998;56:9–21.
- Ensslen-Craig SE, Brady-Kalnay SM. Receptor protein tyrosine phosphatases regulate neural development and axon guidance. *Dev Biol* 2004;275:12–22.
- Brady-Kalnay SM. Protein tyrosine phosphatases. In: Beckerle M, editor. *Cell adhesion: frontiers in molecular biology*. Oxford (UK): Oxford University Press. p. 217–58.
- Brady-Kalnay SM, Mourton T, Nixon JP, et al. Dynamic interaction of PTP $\mu$  with multiple cadherins *in vivo*. *J Cell Biol* 1998;141:287–96.
- Besco J, Popesco MC, Davuluri RV, Frostholm A, Rotter A. Genomic structure and alternative splicing of murine R2B receptor protein tyrosine phosphatases (PTP $\kappa$ ,  $\mu$ ,  $\rho$  and PCP-2). *BMC Genomics* 2004;5:14.
- Brady-Kalnay SM, Flint AJ, Tonks NK. Homophilic binding of PTP  $\mu$ , a receptor-type protein tyrosine phosphatase, can mediate cell-cell aggregation. *J Cell Biol* 1993;122:961–72.
- Gebbink MF, Zondag GC, Wubbolts RW, Beijersbergen RL, van Etten I, Moolenaar WH. Cell-cell adhesion mediated by a receptor-like protein tyrosine phosphatase. *J Biol Chem* 1993;268:16101–4.
- Sap J, Jiang YP, Friedlander D, Grumet M, Schlessinger J. Receptor tyrosine phosphatase R-PTP $\kappa$  mediates homophilic binding. *Mol Cell Biol* 1994;14:1–9.
- Cheng J, Wu K, Armanini M, O'Rourke N, Dowbenko D, Lasky LA. A novel protein-tyrosine phosphatase related to the homotypically adhering  $\kappa$  and  $\mu$  receptors. *J Biol Chem* 1997;272:7264–77.
- Brady-Kalnay SM, Tonks NK. Identification of the homophilic binding site of the receptor protein tyrosine phosphatase PTP $\mu$ . *J Biol Chem* 1994;269:28472–7.
- Del Vecchio RL, Tonks NK. The conserved immunoglobulin domain controls the subcellular localization of the homophilic adhesion receptor protein-tyrosine phosphatase  $\mu$ . *J Biol Chem* 2005;280:1603–12.
- Zondag GC, Koningstein GM, Jiang YP, Sap J, Moolenaar WH, Gebbink MF. Homophilic interactions mediated by receptor tyrosine phosphatases  $\mu$  and  $\kappa$ . A critical role for the novel extracellular MAM domain. *J Biol Chem* 1995;270:14247–50.
- Cismasiu VB, Denes SA, Reilander H, Michel H, Szedlacsek SE. The MAM (meprin/AS-protein/PTP $\mu$ ) domain is a homophilic binding site promoting the lateral dimerization of receptor-like protein-tyrosine phosphatase  $\mu$ . *J Biol Chem* 2004;279:26922–31.
- Aricescu AR, Hon WC, Siebold C, Lu W, van der Merwe PA, Jones EY. Molecular analysis of receptor protein tyrosine phosphatase  $\mu$ -mediated cell adhesion. *EMBO J* 2006;25:701–12.
- Aricescu AR, Siebold C, Choudhuri K, et al. Structure of a tyrosine phosphatase adhesive interaction reveals a spacer-clamp mechanism. *Science* 2007;317:1217–20.
- Besco JA, Hooft van Huijsduijnen R, Frostholm A, Rotter A. Intracellular substrates of brain-enriched receptor protein tyrosine phosphatase  $\rho$  (RPTP $\rho$ /PTPRT). *Brain Res* 2006;1116:50–7.
- Brady-Kalnay SM, Rimm DL, Tonks NK. Receptor protein tyrosine phosphatase PTP $\mu$  associates with cadherins and catenins *in vivo*. *J Cell Biol* 1995;130:977–86.
- Hiscox S, Jiang WG. Association of PTP $\mu$  with catenins in cancer cells: a possible role for E-cadherin. *Int J Oncol* 1998;13:1077–80.
- Zondag GC, Reynolds AB, Moolenaar WH. Receptor protein-tyrosine phosphatase RPTP $\mu$  binds to and dephosphorylates the catenin p120(ctn). *J Biol Chem* 2000;275:11264–9.
- Cavallaro U, Christofori G. Cell adhesion and signalling by cadherins and Ig-CAMs in cancer. *Nat Rev Cancer* 2004;4:118–32.
- Zhang X, Guo A, Yu J, et al. Identification of STAT3 as a substrate of receptor protein tyrosine phosphatase T. *Proc Natl Acad Sci U S A* 2007;104:4060–4.
- Higuchi R, Krummel B, Saiki RK. A general method of *in vitro* preparation and specific mutagenesis of DNA fragments: study of protein and DNA interactions. *Nucleic Acids Res* 1988;16:7351–67.



# Molecular Cancer Research

## Tumor-Derived Extracellular Mutations of PTPRT/PTP $\rho$ Are Defective in Cell Adhesion

Jianshi Yu, Scott Becka, Peng Zhang, et al.

*Mol Cancer Res* 2008;6:1106-1113.

**Updated version** Access the most recent version of this article at:  
<http://mcr.aacrjournals.org/content/6/7/1106>

**Cited articles** This article cites 24 articles, 14 of which you can access for free at:  
<http://mcr.aacrjournals.org/content/6/7/1106.full#ref-list-1>

**Citing articles** This article has been cited by 5 HighWire-hosted articles. Access the articles at:  
<http://mcr.aacrjournals.org/content/6/7/1106.full#related-urls>

**E-mail alerts** [Sign up to receive free email-alerts](#) related to this article or journal.

**Reprints and Subscriptions** To order reprints of this article or to subscribe to the journal, contact the AACR Publications Department at [pubs@aacr.org](mailto:pubs@aacr.org).

**Permissions** To request permission to re-use all or part of this article, use this link  
<http://mcr.aacrjournals.org/content/6/7/1106>.  
Click on "Request Permissions" which will take you to the Copyright Clearance Center's (CCC) Rightslink site.